Aquaculture 572 (2023) 739531

Contents lists available at ScienceDirect

Aquaculture

journal homepage: www.elsevier.com/locate/aquaculture

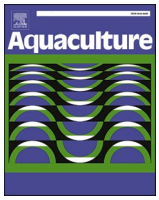

Moritella viscosa early infection and transcriptional responses of intraperitoneal vaccinated and unvaccinated Atlantic salmon

Christian Karlsen [a,*], Elisabeth Ytteborg [a], Anette Furevik [b], Lene Sveen [a], Siv Tunheim [b], Sergey Afanasyev [c], Monica Gausdal Tingbø [b], Aleksei Krasnov [a]

[a] Nofima, Osloveien 1, 1430 Aas, Norway
[b] Pharmaq part of Zoetis, Harbitzalléen 2A, 0275 Oslo, Norway
[c] M. Sechenov Institute of Evolutionary Physiology and Biochemistry, Torez 44, Saint-Petersburg 194223, Russia

ARTICLE INFO

Keywords:
Atlantic salmon
Moritella viscosa
Skin
Ulceration
Vaccination

ABSTRACT

Skin is the first line of defence against waterborne pathogens, such as *Moritella viscosa*, which is the causative agent of winter ulcer disease in Atlantic salmon (*Salmo salar* L.). The present study revealed that vaccination protects against both *M. viscosa*-induced mortality and skin ulceration, but protection varied according to the strain used in the vaccine formulation. Examination of skin tissue 4 days post *M. viscosa* challenge indicated that *M. viscosa* initiated infection by colonising the scale surface. Sequencing the transcripts of the variable region of the IgM heavy chain did not detect effect of vaccination or *M. viscosa* challenge on antibody repertoire and B cell trafficking from the lymphatic organs to skin. Skin layer-specific responses were examined with 44 K oligonucleotide microarray. Skin responded to vaccination and *M. viscosa* challenge by increasing transcription of structural genes, stimulating metabolism, and regulation of developmental processes. Immune responses to dead (vaccine) and live *M. viscosa* were very similar and no pathogen-specific changes were found. Combined use of skin transcriptional profiles and image analysis revealed differences in the infected skin layers between the study groups. *M. viscosa* was likely retained in the epidermis of vaccinated salmon, whereas the dermis was colonised in unvaccinated fish. Furthermore, decreased expression of lymphocyte-specific and antiviral genes in the dermis indicated possible evasion of immune-related cells from skin in salmon challenged with *M. viscosa*. Our data also indicated that intraperitoneal vaccination may prime the humoral innate response, which enables a rapid response in the dermis layer of skin during *M. viscosa* invasion.

1. Introduction

Outbreaks of ulcerative disease in farmed Atlantic salmon (*Salmo salar* L.) occur across the North Atlantic region, and numerous bacterial species have been isolated from ulcerated fish (Benediktsdottir et al., 1998; Bruno et al., 1998; Benediktsdottir et al., 2000; Lunder et al., 2000; Whitman et al., 2000; Olsen et al., 2011). Experimentally, skin ulcers and mortality due to infection have been verified from *Moritella viscosa* (Lunder et al., 1995), *Tenacibaculum finnmarkense* (Småge et al., 2018), and *Aliivibrio wodanis* (Karlsen et al., 2014b). Ulcerative outbreaks below seawater temperatures of 8 °C, termed classic winter ulcer disease, commonly refer to infection with the bacterium *M. viscosa*. The disease manifests with symptoms of superficial skin lesions that develop into larger, chronic skin ulcers and degenerative changes in the underlying muscle tissue, followed by terminal septicaemia (Lunder et al., 1995). The extracellular products of *M. viscosa* are cytotoxic to fish cells and lethal to Atlantic salmon (Bjornsdottir et al., 2009; Bjornsdottir et al., 2011), with several predicted toxin-related homologs and virulence factors (Tunsjø et al., 2011; Karlsen et al., 2014a). Two major phenotypic and genotypic clades (classic and variant) have been identified in *M. viscosa* (Grove et al., 2010) with different host-specific virulence (Karlsen et al., 2014a). Genome analyses have shown that the genome properties among *M. viscosa* are linked to strain relationships (Karlsen et al., 2017a). This may suggest that lineages within *M. viscosa* have evolved both antigenic and virulence variance. The clinical diagnostic overview for isolates characterised from Norwegian farmed Atlantic salmon has recently changed. A genetic shift in the dominant sub-populations of *M. viscosa* is observed where the earliest homogenous related classic *M. viscosa* is no longer the dominating genotype (Sommerset et al., 2021).

* Corresponding author.
E-mail address: Christian.karlsen@nofima.no (C. Karlsen).

https://doi.org/10.1016/j.aquaculture.2023.739531
Received 8 November 2022; Received in revised form 26 February 2023; Accepted 27 March 2023
Available online 29 March 2023

Several intraperitoneally (i.p.) administered oil-adjuvanted polyvalent vaccines are currently available and used in commercial aquaculture against *M. viscosa* (Karlsen et al., 2017b). Although challenge models have confirmed specific protection against disease development, they have also revealed differences in vaccine efficacy (Karlsen et al., 2017b). *M. viscosa* have different serotypes (Heidarsdóttir et al., 2008), and strains from Norwegian winter-ulcer outbreaks can be separated into several genotype sub-populations (Sommerset et al., 2021), which in part, could explain the persistence of outbreaks in vaccinated salmon during production.

Once a vaccine is administrated, the process of eliciting an immune response with memory is initiated through the activation of B cells that will produce antigen-specific immunoglobulins (Igs) that in turn, will help identify and neutralise foreign objects. Among the three teleost types of Ig, IgM is the predominant type in Atlantic salmon, which plays a key role in systemic responses (Makesh et al., 2015; Piazzon et al., 2016; Jenberie et al., 2018). Sequencing of the variable region of IgM heavy chain transcripts (Ig-seq) has been used to assess the diversity and size of the antibody repertoire, detect responses to immunisation, and examine B cell trafficking between tissues (Castro et al., 2017; Krasnov et al., 2017; Bakke et al., 2020). However, further studies are required to examine the mechanisms of vaccine protection against the development of skin ulceration and mortality. It is unclear how the different layers of the skin, including the outer epidermis, which is covered by a mucosal layer, and the deeper vascularised dermis layers, respond to i.p. immunisation and host–pathogen interactions. Each skin layer is composed of different cell types that play important roles in protection and regeneration after damage, as previously reviewed (Sveen et al., 2020). The epidermis is the first line of defence and consists of live cells (e.g. keratocytes and mucus cells) that can immediately respond to environmental changes, including environmental challenges and pathogen exposure. The scales provide the skin with further armor and strength to withstand mechanical pressure, while the dermis makes the skin more flexible and elastic through the dense, irregular connective tissue. A better understanding of the potential of i.p. inactivated vaccines with the use of adjuvants to induce immunity in the skin will help development towards inducing appropriate responses against challenging Atlantic salmon pathogens.

The present study used microscopy combined with Ig and transcriptome analyses to study host–microbial interactions in the skin of unvaccinated and vaccinated Atlantic salmon during an experimental challenge using a variant isolate of *M. viscosa*. Vaccination was performed by i.p. injection using monovalent experimental vaccines containing either classic or variant *M. viscosa* isolate and indicated that the use of different strains of *M. viscosa* influenced the efficacy of the vaccine. Skin samples from fish vaccinated against only classic *M. viscosa* were used for further analyses. Our results suggest that *M. viscosa* infects the epidermis of vaccinated salmon and the deeper dermis layer in unvaccinated salmon. Although vaccination and bacterial challenge induced similar changes in the dermis, its effects on the antibody repertoire and immune gene expression were limited.

2. Material and methods

2.1. Bacterial isolates used for vaccine preparation and challenge

Isolates of *M. viscosa* used for vaccine formulation and challenge were collected as submissions to the bacteriology laboratory at Pharmaq (Norway). The isolates were sampled from winter ulcer outbreaks in Norwegian Atlantic salmon and confirmed to be *M. viscosa* using a commercial slide agglutination kit (Bionor) and *gyrB* sequencing adapted from previously described methods (Grove et al., 2010). Genomic DNA was isolated from single colonies on blood agar plates using the InstaGene Matrix (Bio-Rad) according to the manufacturer's instructions. The partial *gyrB* gene was amplified and sequenced using forward primer AGG TGG TTT ACA CGG TGT TGG TG and reverse primer GCA CCA CGG AAA CCA GCA AGG. The primers were designed in Primer-BLAST (Ye et al., 2012) based on a subset of available sequences of *M. viscosa* and *Moritella marina* attained from GenBank. Gene amplification was performed using a S1000 Thermal cycler (Bio-Rad), and each 25-μL reaction was prepared using PuReTaqReady-To-Go PCR beads (GE healthcare). The PCR reaction was performed as follows: one cycle of 94 °C for 5 min, 35 cycles of 94 °C for 20 s, 55 °C for 30 s and 72 °C for 50 s, and one cycle of 72 °C for 7 min. Amplicons were sequenced at LGC Genomics Ltd. Sequences were compiled using the CLC Main Workbench version 8.0 (Qiagen) and aligned using ClustalW prior to neighbour-joining analysis using MEGA 7.0 software. Ambiguous bases were excluded from the analysis. Bootstrap confidence values were obtained with 500 re-samplings.

Two experimental monovalent vaccines were prepared as water-in-oil formulations using a formaldehyde-inactivated classic or variant strain of *M. viscosa*. Both vaccines were blended to contain equal concentrations of antigen. The water phase, which contains the antigens, was dispersed into a mineral oil phase (continuous phase containing emulsifiers and stabilizers).

Challenge material homologous to the variant *M. viscosa* used in one of the vaccines was freshly cultivated from a frozen bacterial stock in shake flask culture medium based on yeast extract at 12 °C for two days with shaking.

2.2. Fish vaccination and infection challenge

The present study was performed at the Industrial and Aquatic Laboratory (ILAB, Bergen, Norway) and included 130 unvaccinated Atlantic salmon (mean weight of 30 g). The study was approved by the Norwegian Food Safety Authority and conducted in accordance with the regulations controlling experiments and procedures for live animals in Norway.

The fish and tank environmental parameters were monitored daily with a biomass density below the maximum acceptable limit of 40 kg/m^3 in flow-through systems for salmonids. Fish were fed daily according to their appetite throughout the study, except for 24 h prior to vaccination and *M. viscosa* challenge, when the fish were starved. For vaccination with oil-adjuvanted formalin-inactivated *M. viscosa*, the fish were randomly removed from the holding tanks and anesthetised using tricaine 80 mg/L before being marked (by cutting the right maxillae or adipose fin) and i.p. vaccinated (V+) or injected with phosphate-buffered saline (PBS; V-) administered at a dose volume of 0.05 mL per fish using calibrated pistol grip syringes. The fish were transferred to 500-L immunisation tanks and immunised for 1574 degree-days prior to bacterial challenge. A continuous photoperiod of LD24:0 was used 5 weeks prior transfer to the disease facility. The fish were acclimatised to 8 °C and 34‰ salinity prior to the challenge. Three tanks were used, each containing vaccinated and PBS-treated fish. Two tanks were used to investigate responses 4 days post-infection (dpi), including the sham-exposed time-matched control, and one tank was used to assess cumulative mortality after infection. Fish were subjected to a 1-h bath challenge using a freshly cultivated *gyrB* variant Atlantic salmon isolate of *M. viscosa* isolated from an outbreak in the northern production area of Norway. Adequate environmental parameters were ensured by oxygenation and aeration during the challenge. Mortality was recorded daily during the challenge period, which was terminated at day 28 post infection. Extensive ulceration was observed on all fish that died during the study period. For ethical reasons, ulcerated or moribund fish were euthanised by tricaine overdose and recorded as mortalities. At the end of the study period, all surviving fish were euthanised by tricaine overdose, counted by group, and cutaneous lesions were scored in all survivors from each tank using a previously described scoring system (Karlsen et al., 2017b). Briefly, each survivor was visually inspected and categorised according to score as follows: 0, no visible lesions; 1, at least one superficial skin lesion not permeating the basement membrane or swelling of scale pockets and superficial skin oedema; and 2, formation

of at least one severe ulcer permeating the basement membrane. Individuals categorised as score 2 were included in the final mortality graph.

2.3. Sampling procedure

Fish were grouped according to treatment as follows: V-Mv-, not vaccinated and not challenged with *M. viscosa* (control); V-Mv+, not vaccinated and challenged with *M. viscosa*; V+Mv-, vaccinated and not challenged with *M. viscosa*; and V+Mv+, vaccinated and challenged with *M. viscosa*. Six fish per group were sampled at 4 dpi after being euthanised by a tricaine overdose. Intact skin from the two non-challenged groups was sampled by excising pieces from the left side of each fish in the area posterior of the dorsal fin and above the lateral line and immediately fixated as described below. In the two challenged groups, initial skin ulcer areas, observed as raised scales, were sampled above the lateral line for transcriptional analysis while initial skin ulcer areas for image analysis also included samples below the lateral line. Sections of the gill, spleen, and head kidney were aseptically removed and immediately fixed. Samples for histology were placed in 20-mL pots containing 10% buffered formalin (CellStor, CellPath) and stored at 4 °C. Samples for scanning electron microscopy (SEM) analyses were stored in 4% glutaraldehyde (Sigma Aldrich) 0.1 M sodium phosphate buffer and stored at 4 °C. Samples for RNA analysis were stored in RNAlater (Invitrogen), kept cool during transport, and stored at −80 °C until used for RNA extraction.

2.4. Histological staining

Samples fixed in buffered formalin were carefully dissected, orientated, and placed in a tissue-embedding cassette (Simport). Tissue processing was performed using an automated tissue processor (TP1020, Leica Biosystems) in which samples were dehydrated using a graded series of ethanol (up to 100%), followed by a clearant xylene bath and infiltration in melted paraffin at 60 °C (Merck). Paraffin-embedded tissue samples were cut to 5-μm sections using a Microtome (Leica RM 2165), mounted on polysinecoated slides (Avantor), and dried overnight at 37 °C. The sections were deparaffinised and rehydrated, and staining was performed using an automated stainer (Autostainer XL Leica Biosystems). Paraffin sections were stained using Alcian Blue Periodic Acid Schiff (AB/PAS, pH 2.5, Alcian Blue 8GX, Sigma Aldrich). Slides were examined using a light microscope slide scanner (Leica Microsystems) and evaluated using an Aperio Image Scope (Leica). The thickness of the epidermis was measured in μm using tools in Aperio. The total number of mucus-producing cells, as well as their different colours (pink or blue), were counted, and mucous cells per 100 μm of epidermis and the ratio of pink/total mucous cell calculated. In addition, mucous cell distribution in the epidermis (mucous cells touching the outer surface of the epidermis were defined as "outer") were counted, and ratio of outer/total mucous cells calculated.

2.5. Scanning electron microscopy

Samples fixed in 4.0% glutaraldehyde 0.1 M sodium phosphate buffer for SEM were gently washed in PBS, dehydrated in a graded series of ethanol up to 100%, and dried using a critical point dryer (CPD 030, Bal-tec AG) with liquid carbon dioxide as the transitional fluid. The samples were mounted on stubs with carbon tape and coated with gold–palladium (Polaron Emitech SC7640 Sputter Coater, Quorum technologies) and examined using SEM (Zeiss EVO-50–EP, Carl Zeiss).

2.6. Immunohistochemistry

Samples were prepared as described in the Histological staining section. In brief, immunohistochemistry (IHC) was performed by blocking with horse serum (Sigma) for 20 min, followed by 30 min with rabbit antiserum raised against *Moritella* isolate NVI 478/88 (Lunder et al., 1995). Slides were washed twice in PBS before incubating with ImmPress AP-anti-Rabbit IgG (Vector Laboratories) for 30 min. Immpact Vector Red substrate kit (Vector Laboratories) with alkaline phosphatase was used for 30 min according to the protocol before counterstaining 30 s with haematoxylin (Sigma). All slides were scanned using a Leica slide scanner and the Aperio images system and analysed using Zeiss Axio Observer Z1 equipped with AxioVision software (Carl Zeiss Microimaging).

2.7. Separation of skin layers and RNA extraction

Skin layer dissection was performed under a microscope (Leica, Wild M3B). Scales were removed using forceps and placed side up on a sterile petri dish. The epidermis (the outer surface exposed to the environment) was gently scraped off the surface of the tip of six scales using a sterile scalpel blade and collected into tubes prefilled with Lysis LBE buffer (Beckman Coulter) for RNA extraction, and the scales were then discarded. Any traces of subcutaneous tissue (adipose and muscle tissue) were scraped off the remaining skin sample and transferred to separate prefilled Lysis LBE buffered tubes. The tissue layer collected using this method was defined as the dermis. Total RNA was extracted from the epidermis and dermis of the skin, gills, spleen, and head kidney using an automated Biomek 4000 (Beckman Coulter), including an on-column DNase treatment according to the manufacturer's protocol. RNA integrity number ≥ 7.5 was used as cutoff value for utilisation of sample for transcriptome analysis and was measured using a 2100 Bioanalyzer and RNA Nano Chips (Agilent Technologies) before RNA purity and concentration were measured using a NanoDrop ND-1000 Spectrophotometer (NanoDrop Technologies). RNA samples were stored at −80 °C.

2.8. Ig-seq

Parallel sequencing of V(*D*)J junction (CDR3) is used for characterization of the IgM repertoire. Each unique sequence marks clonal B cells and the number of reads shows the size of clonotype. Increased cumulative frequency of hundred largest clonotypes (CF100) indicates recent expansion of B cells clones. Co-occurrence of clonotypes in tissues from the same fish reflects migration of B cells. Synthesis of cDNA was primed with oligonucleotide to the constant region of the heavy chain of Atlantic salmon IgM (TAAAGAGACGGGTGCTGCAG) using SuperScript IV reverse transcriptase (Thermofisher Scientific) according to the manufacturer's instructions. A degenerate primer TCGTCGGCAGCGTCAGATGTGTATAAGAGACAGTGARGACWCWGCWGTGTATTAYTGTG aligning to the 3′-end of all Atlantic salmon VH genes and a primer GTCTCGTGGGCTCGGAGATGTGTATAAGAGACAGGGAACAAAGTCGGAGCAGTTGATGA aligning to the 5′-end of the constant regions were used for PCR amplification of cDNA. Reaction mixtures (20 μL) included 10 μL of 2× Platinum Hot Start PCR Master Mix (Thermofisher Scientific), 0.5 μL of each primer (10 pmol/μL), 8 μL of water, and 1 μL of template. A second PCR was performed using Illumina Nexter XT Index Kit v2, with the reaction including 2 μL of each primer and 2 μL of product of the first PCR. The PCR program included heating for 1 min at 94 °C, amplification for 10 s at 94 °C, 20 s at 53 °C, and 20 s at 72 °C (30 cycles in the first PCR and nine cycles in the second PCR), and extension for 5 min at 72 °C. DNA concentration was measured using Qubit (Thermofisher Scientific). Aliquots of libraries were combined and purified twice using the Qiagen PCR clean-up kit. Sequencing was performed using the Illumina MiSeq Reagent Kit v3 (150-cycle). Libraries were diluted to 4 nM, and PhiX control was added to a concentration of 0.8 nM. Illumina adaptors and primers were trimmed, low-quality reads were removed, and the sequences were transferred to a database. The study groups were compared by CF100. Two metrics were determined to assess co-occurrence of clonotypes in issues: the number of leaders from tissue 1 also detected in tissue 2 with a frequency $> 10^{-4}$ and the number of leaders from tissue 2 also detected in tissue 1.

2.9. Microarray analysis

Microarray analyses were carried out on both skin layers from six fish each in the four groups using Nofima's Atlantic salmon genome-wide 44 K DNA oligonucleotide microarray, Salgeno-2 (GPL28080), totally 48 samples were analysed. The microarrays were manufactured by Agilent Technologies and the reagents and equipment were purchased from the same provider. RNA amplification and labelling were performed using a One-Colour Quick Amp Labelling Kit, and a Gene Expression Hybridization kit was used for fragmentation of labelled RNA. The total RNA input for each reaction was 500 ng. After overnight hybridisation in an oven (17 h, 65 °C, rotation speed 0.01 × *g*), the arrays were washed with Gene Expression Wash Buffers 1 and 2 and scanned using a microarray scanner (SureScan, Agilent Technologies).

2.10. Statistical analysis

Differences in mortality between treatments were determined using Kaplan–Meier analysis and applying the log-rank test. Lesion score data were analysed using Kruskal–Wallis test followed by Steel–Dwass post hoc tests for pairwise ranking to compare the groups. Group means were tested by *t*-test to compare parametric data obtained from histological images. Ig-seq data were analysed using ANOVA followed by Tukey's post-hoc test. Global normalisation of gene transcription data was accomplished by equalising the mean intensities of all microarrays. The individual values for each feature were divided by the mean value of all the samples to produce expression ratios (ERs). The log2-ER was calculated and normalised using the locally weighted non-linear regression (Lowess). Differentially expressed genes (DEGs), represented by differently expressed probes on the array, were selected using criteria of 1.75-fold change and $P < 0.05$. STARS annotations were used for comparison of the functional groups of genes (mean log2-ER, *t*-test). Gene expression data were processed and analysed using Nofima's bioinformatics package (Krasnov et al., 2011). Statistical analysis of other data was performed using commercial software, including GraphPad Prism v.8 and JMPPro v13.1.0.

3. Results

3.1. Mortality and lesion scores

Extensive ulceration was observed on all fish that died during the study period. Fish categorised as lesion score 2 at termination of the trial were included in the final mortality graph. The cumulative mortality in the PBS-treated control group was 73%. Significant ($P = 0.0288$: log-rank test) protection was observed in fish vaccinated against both variant and classic *M. viscosa* isolate (Fig. 1). Vaccine formulated with the *gyrB*-variant isolate performed better (cumulative mortality of 11%) than that formulated with the *gyrB*-classic isolate, which had a cumulative mortality of 31%.

3.2. Imaging of initial colonisation and tissue response

Skin from the groups not challenged with *M. viscosa* (V-Mv-/V+Mv-) showed normal morphology with intact epidermis, scales, and loose connective tissue (Fig. 2). The epidermis was thinner towards the tip of the scales, which was typically observed in healthy fish (Fig. 2B). However, skin from fish in the V+Mv- (vaccinated, unchallenged) group showed an increase in mucous cells located in the outermost epidermis (measured as the ratio of outer mucous cells/total number of mucous cells) (Fig. 2E).

Following *M. viscosa* challenge, the epidermis of fish in the V-Mv+ and V+Mv+ groups showed an increase in thickness at the tip of the scales, giving the epidermis a rounder appearance, while the scales developed a curly structure (Fig. 2D). Although intact skin from fish in the V+Mv+ group showed no difference in overall morphology, fish in the V+Mv+ group had fewer mucous cells at the outer border of the epidermis than those in the V-Mv+ group (Fig. 2F), with purple mucous cells observed at the outer surface of the epidermis. Skin areas without ulcers from fish in the *M. viscosa*-challenged groups (V-Mv+/V+Mv+) compared to those not challenged with *M. viscosa* (V-Mv-/V+Mv-) had increased epidermal thickness and number of mucous cells (Fig. 2G, H).

Fish challenged with *M. viscosa* (V-Mv+/V+Mv+) showed a more disrupted skin structure with visible wounds. The skin of fish with mild symptoms showed curly scales (Fig. 2I) with thicker epidermis and damaged, loose connective tissue. All layers of the skin were affected in fish with more pronounced wound development (Fig. 2J–L), including

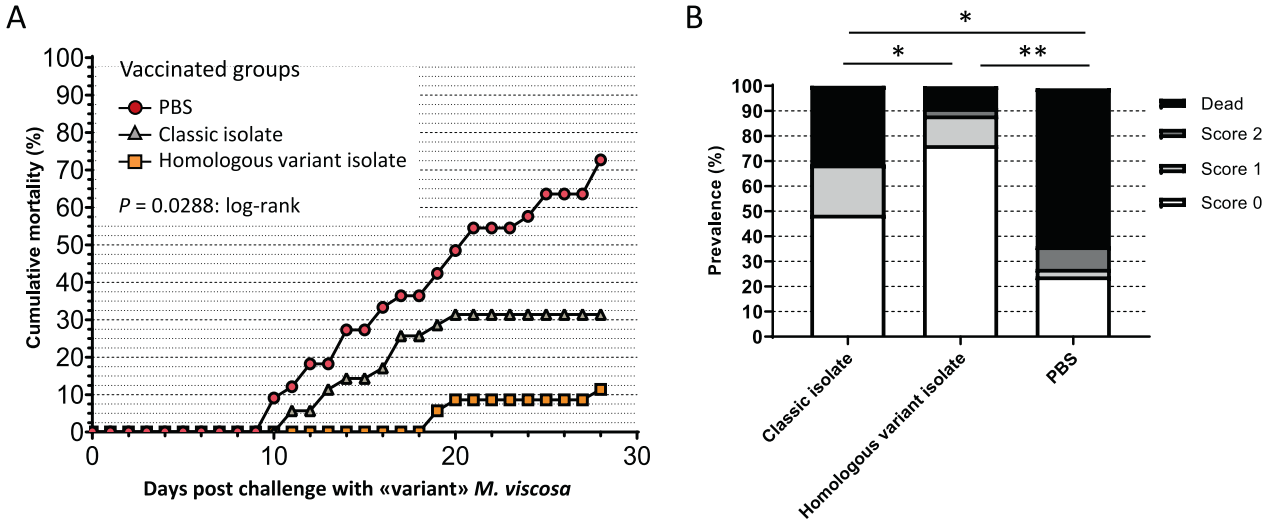

Fig. 1. Cumulative mortality (A) and ulceration (B) of Atlantic salmon vaccinated groups after bath challenged with variant *M. viscosa*. (A) Cumulative mortality (%) between treatment groups intraperitoneal vaccinated with either PBS, classic isolate of *M. viscosa* or a homologous isolate of *M. viscosa* was significant different ($P = 0.0288$: log-rank test). At termination, fish with a lesion score of 2 were included in the mortality count, as shown by the increase in mortality at the end of the study in the PBS-vaccinated fish. (B) Combined mortality and lesion scores at termination of the trial. Significant differences between groups are indicated. * $P \leq 0.05$, ** $P \leq 0.001$ (Kruskal–Wallis and Steel–Dwass multiple comparisons test).

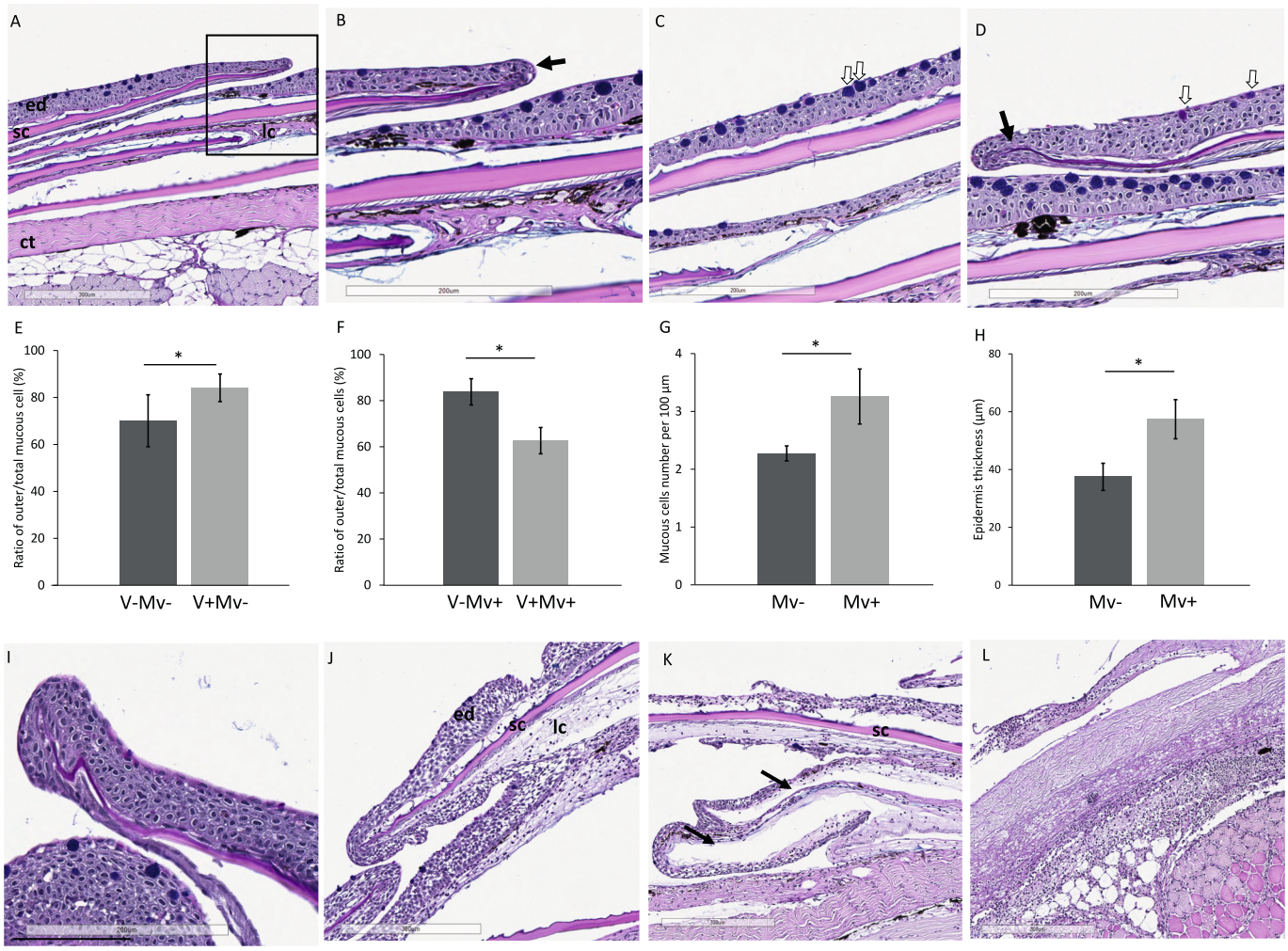

Fig. 2. AB/PAS histological staining of Atlantic salmon skin from (A) fish in the V-Mv- group, which showed a normal skin morphology. The enlarged box in (B) shows a thin layer of epidermis covering the tip of the scale (arrow). (C) Fish in the V+Mv- group showed a similar skin morphology to the V-Mv- group, but with more mucous cells (hollow arrows) in the outer epidermis. (D) Bacterially challenged fish in both the unvaccinated and vaccinated groups (V-Mv+/V+Mv+) showed thickening of the epidermis around the tip of the scales (arrow), purple mucous cells (hollow arrow), and curving of the scales. (E) The ratio of mucous cells in the outer epidermis was increased in vaccinated fish. (F) The ratio of mucous cells in the outer epidermis was decreased in fish in the V+Mv+ group. Intact skin of fish challenged with *M. viscosa* (V-Mv+/V+Mv+) showed an increase in both (G) mucous cell number and (H) thickness of the epidermis. Fish with visible *M. viscosa*-induced wounds (V-Mv+/V+Mv+) had severely increased epidermal thickness around curled scales in the regions with intact epidermis (I) and disintegrated loose connective tissue and vacuolisation of epithelial tissue combined with immune-related cell infiltration in the scale pockets (J). Disintegrated scale pockets were also accompanied by scale loss (K, arrow) and severe damage of the skin structures and the underlying tissue, with loss of epithelial tissue and scales, combined with immune-related cell infiltration in subcutaneous tissue and necrotic muscle fibres (L). * $P < 0.05$, *t*-test ($n = 24$). (For interpretation of the references to colour in this figure legend, the reader is referred to the web version of this article.)

vacuolisation of keratocytes, loss of epithelial tissue, disintegrated or loss of scales, invasion of immune-related cells, and disintegrated connective tissue.

SEM images of macroscopic swelling skin areas infected by *M. viscosa* (Fig. 3) showed disintegration of epithelial tissue, typically with loss of the distinct morphological features of the surface keratocytes, such as their pentagonal shape and microridges (exemplified in Fig. 3A), accompanied by complete disintegration and holes in the epithelial tissue (Fig. 3B and F). Scales were exposed in areas where the epithelial tissue was missing and frequently displayed bacteria on the scale surfaces (Fig. 3C-E). The bacteria were either found in small clusters (Fig. 3H, and I), suggesting new colonies, or more extensive colonisation with bacteria covering the entire surface of the fish scales (Fig. 3G). Infiltration of white and red blood cells was prominent in heavily infected areas (Fig. 3E, K), both in the scale pocket and the connective tissue compartment between the epidermis and the scales, and in direct contact with *M. viscosa*.

IHC using antibodies against *M. viscosa* showed weak staining in fish skin without wounds and intense staining in developed wounds. Positive staining was detected in both the V-Mv+ and V+Mv+ groups with no visible wounds, and the initial staining was limited to the area between the epidermis and the top of the scales, with the grade of staining varying between samples (Fig. 4A and B). Staining was more intense in skin samples with more developed wounds with immune-related cell invasion and disrupted loose connective tissue (Fig. 4C). Staining was also observed in developed wounds in the scale pockets at both sides of the scales. Most of the skin structures were lost in the wound centre, and intense, positive staining was observed in the remaining tissue. Furthermore, skin tissue layer infection differed between the V-Mv+ and V+Mv+ groups. While unvaccinated fish with wounds showed more intense staining in the dermis (Fig. 4D–F), vaccinated fish showed positive staining in the epidermis and loose connective tissue around the scales (Fig. 4G–I).

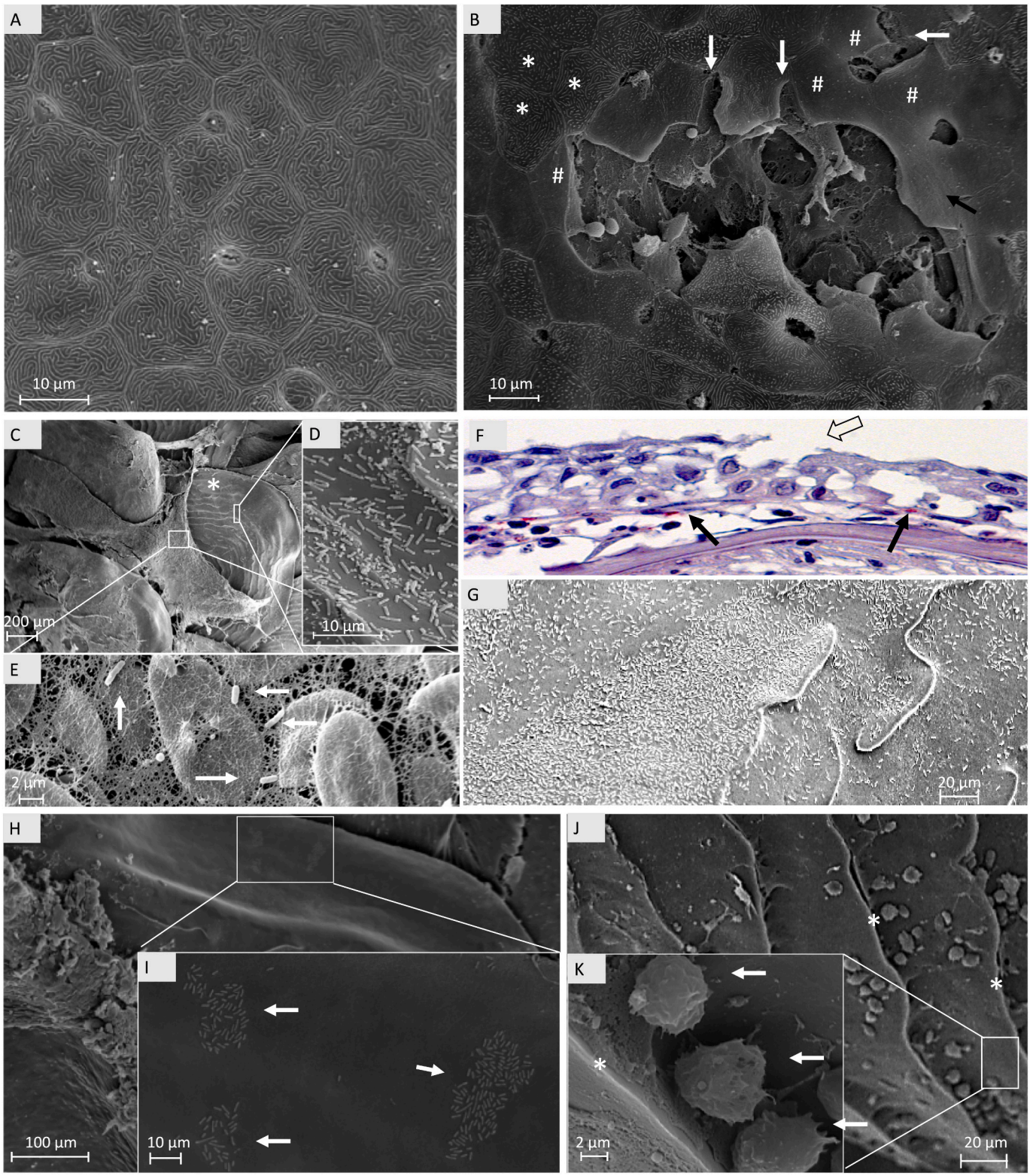

Fig. 3. Images of Atlantic salmon skin 4 days post *M. viscosa* infection. (A) Intact skin with pentagonal shaped keratocytes with microridges. (B) Example of skin surface with deterioration of the epidermis from within. Keratocytes with loss of microridges (#) at the wound edge break the cell-to-cell adhesion and detach (arrows), leaving a "hole" in the epithelial tissue, which is in strong contrast to the intact epidermal surface displaying pentagonal shaped keratocytes with microridges (*). (C) Macroscopic swelling of the skin shows surface with exposed scale (*). (D) Higher magnification of the scale shown in (C) revealing colonisation of the scale surface by *M. viscosa*, followed by (E) an inverted scale pocket infiltrated with blood cells and bacteria (arrows). (F) IHC of the epidermal layer showing *M. viscosa* located in the scale pocket in red (arrow) and deterioration of the epithelial tissue displaying a hole (hallow arrow) in the epidermal surface, as observed in (B). (G) Excessive colonisation of the scale surface. (H) Scale surface at a higher magnification (I) showing colonising clusters of bacteria (arrows). (J) Scale surface with circuli (*) and immune-related cells (arrows), enlarged in (K). (For interpretation of the references to colour in this figure legend, the reader is referred to the web version of this article.)

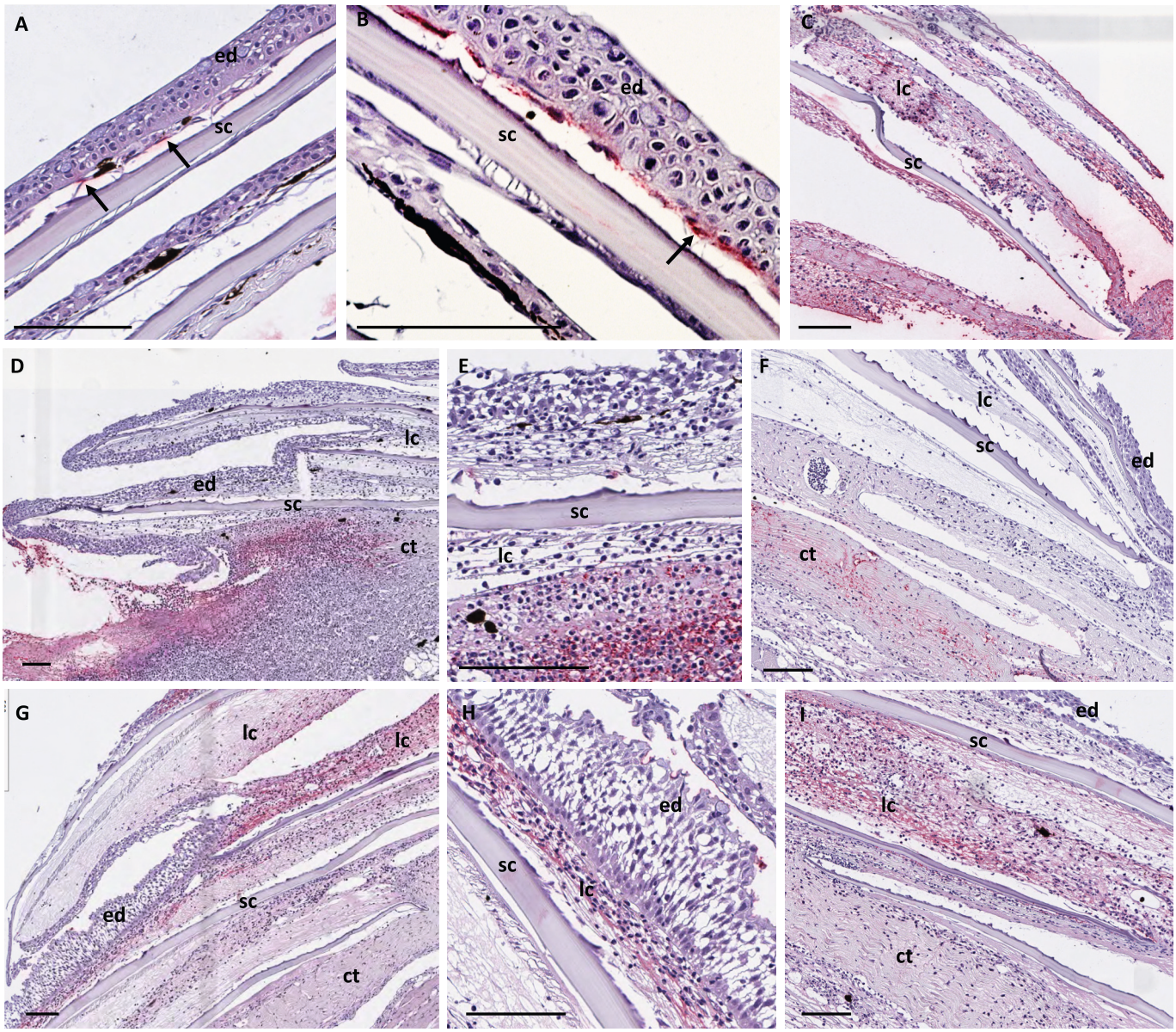

Fig. 4. IHC using *M. viscosa* antibody, with positive staining shown in red (arrow). (A) Positive staining (arrow) was found in both the unvaccinated and vaccinated groups challenged with *M. viscosa* (V-Mv+/V+Mv+), with localisation limited between the epidermis and scales. (B) Some skin samples showed more intense staining in this region. (C) Staining was more evident along the borders of the developed wounds and was also found in the scale pockets and deeper layers of the skin. (D) Unvaccinated *M. viscosa*-challenged (V-Mv+) fish showed staining in the wound centre, which was more intense in the remaining dermis (E and F). (G) Vaccinated fish challenged with *M. viscosa* (V+Mv+) showed staining in the loose connective tissue, as shown at higher magnifications in (H) and (I). Scale bar = 100 μm. Ed, epidermis; sc, scale; lc, loose connective tissue; ct, connective tissue. (For interpretation of the references to colour in this figure legend, the reader is referred to the web version of this article.)

3.3. Ig-seq

Sequencing analysis did not detect effects of vaccination or *M. viscosa* challenge on the IgM repertoire: CF100 and co-occurrence of clonotypes were equal in all study groups. To take advantage of Ig-seq data, IgM repertoires of Atlantic salmon tissues were compared. Large clonotypes were predominant in the peripheral tissues and the 100 largest clonotypes yielded 52% and 73% of the transcripts in gill and skin (dermis), respectively (Table 1). The cumulative frequencies in the lymphatic tissues, head kidney and spleen were lower (22% and 27%, respectively). Thus CF100, which is inversely related to the complexity, suggested a small size of repertoire in the skin with predominance of the largest clonotypes. Co-occurrence of clonotypes reflect the B cells traffic between tissues. The population of B cells in the dermis was the least similar to other tissues: only ~20% of the largest clonotypes were detected elsewhere. Sharing of largest gill clonotypes with the lymphatic organs was twofold greater (38%–39.5%), while the overlap between gill and skin was only 14%. The repertoires of the head kidney and spleen were closer to each other compared with the peripheral tissues. The clonotypes of the lymphatic organs detected in gills was twofold that of skin.

3.4. Transcriptome analyses

3.4.1. Effect of vaccination and challenge with M. viscosa

Differences in the skin transcriptional profiles between the study groups are shown in Fig. 5. Ranking the effect according to the number of DEGs showed that vaccination affected the dermis more than the

Table 1
Percentage cumulative frequencies of the 100 largest clonotypes shared across tissues.

		Tissue distribution			
Tissue	CF100 ± SE	Dermis	Gill	HK	Spleen
Dermis	73.22 ± 1.49		19.7	20.8	20.3
Gill	52.06 ± 1.49	14.2		38.0	39.5
HK	22.24 ± 1.45	7.6	17.2		27.4
Spleen	26.61 ± 1.49	9.0	18.9	31.1	

CF100, cumulative frequency; HK, head kidney; SE, standard error.

epidermis and the response to *M. viscosa* was strongest in the dermis of unvaccinated salmon (Fig. 5A). Vaccination and infection caused similar expression changes in the dermis, as demonstrated by the correlation between vaccinated and *M. viscosa*-challenged groups (Fig. 5B). In the epidermis, comparatively large expression changes were only observed in fish subjected to both treatments (V+Mv+). While the dermis was affected by both vaccination and *M. viscosa* challenge, the epidermis seemed to only respond to the combined treatment with vaccination and *M. viscosa* challenge (V+Mv+) (Fig. 5C).

Several functional gene groups showed coordinated expression changes, with mean values significantly different from the V-Mv- group and only three groups were related to immune responses (Fig. 6A). Decreased expression of virus-responsive genes was observed in all study groups. Reduced levels of transcripts encoding B and T cell-specific genes, including many highly specialised genes, was observed in vaccinated salmon (Fig. 6B). These changes were most likely caused by the evasion of immune-related cells from skin. Apart from this finding, immune responses to vaccination and pathogen challenge were very similar with only a few genes showing significantly stronger activation in V+Mv+. Vaccination and live *M. viscosa* stimulated transcription of a pathogen recognising *toll-like receptor 13* and several proinflammatory genes, including cytokines and signalling molecules (*il1b*, *il21*, *chitinase*, and *granulins*) and effectors (*cytochrome b-245* and a *perforin*-like gene). Activation of eicosanoid metabolism may indicate signalling via lipid mediators. With the exception of antiviral and T cells responses, all the functional groups shown in Fig. 6A were activated. Vaccination and *M. viscosa* challenge increased the expression of genes encoding structural proteins, including both intracellular (cytoskeleton including microtubules) and extracellular (mucus) proteins. These treatments also stimulated diverse processes involved in life support and maintenance of cells, development, repair of tissue, and several metabolic pathways. Similar responses were induced in the dermis and epidermis of vaccinated *M. viscosa*-challenged fish (V+Mv+).

3.4.2. Comparison of epidermis and dermis transcriptional profiles

Statistically significant and greater than twofold differential expression between epidermis and dermis was found for 4439 genes. Differences were observed between several functional groups (Fig. 7). Genes associated with cell proliferation and keratin cytoskeleton were up-regulated in the epidermis along with several genes that play various protective roles, including genes encoding mucus proteins and proteins involved in antigen presentation, innate antiviral responses, T cell-specific genes, and xenobiotic metabolism. Regulators of epidermal morphogenesis (e.g., Wnt) and proteins involved in cell-to-cell adhesion (integrins, nectins, claudins, and cadherins) were also expressed at a higher level in the epidermis. Transcripts with markedly higher expression in the dermis encoded cytoskeleton components, myofiber proteins, and proteins involved in motor activity. Also, mitochondrial proteins and transporters involved in sugar and calcium metabolism were up-regulated. Developmental processes appeared to be more active in the dermis, as indicated by higher expression of growth factors, proteins involved in scale development (pappalysins and periostins), regulators of cell proliferation and differentiation, and genes encoding proteins involved in the extracellular matrix and endothelium. Expression of genes encoding plasma and complement proteins and markers of erythrocytes was also higher in the dermis. The number of genes with dermis-specific expression was markedly larger and a >10-fold difference was shown for 233 genes in the dermis, compared with 19 genes in the epidermis.

4. Discussion

Vaccination resulted in significant protection against both *M. viscosa*-induced mortality and skin ulceration, although protection varied according to the vaccine formulation, corroborating the difference between the classic and variant isolates. This could, in part, be due to the existence of different *M. viscosa* serotypes, as previously suggested (Heidarsdóttir et al., 2008). Although a degree of cross-protection may occur (Greger and Goodrich, 1999), which is further supported by the findings of our study. Our results also suggest that the use of variant *M. viscosa* may be important to improve vaccination against winter ulcers.

Histological and immunohistochemical observations of fish infected with *M. viscosa* showed similar morphologies to those previously described for ulcers (Lunder et al., 1995). We observed early signs of the pathology, including thickening of the epidermis, disintegration of the

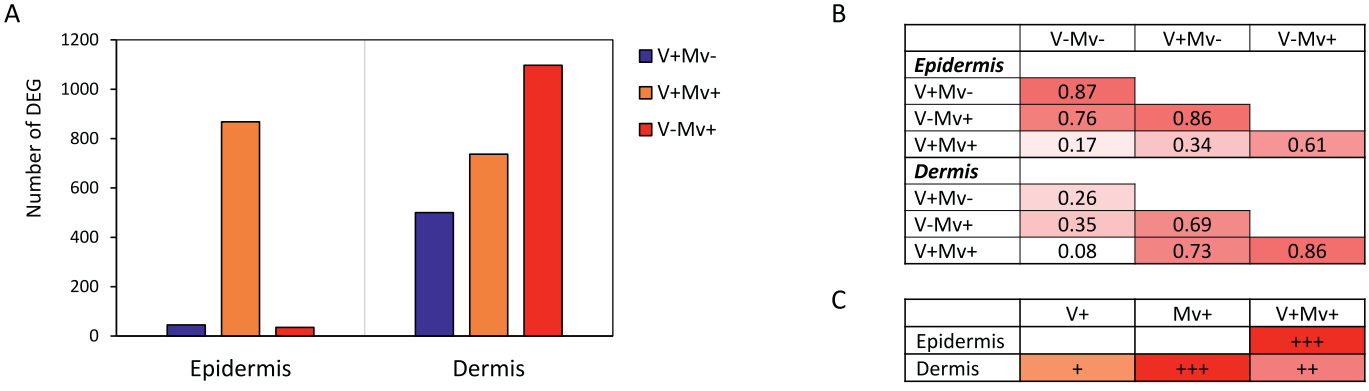

Fig. 5. Microarray analyses of Atlantic salmon skin. (A) The number of differently expressed genes (DEGs) compared with the V-Mv- (unvaccinated fish not challenged with *M. viscosa*) group. (B) Pearson correlation (r) of expression profiles between the groups. (C) Summary of the transcriptional changes caused by vaccination (V+), *M. viscosa* challenge (Mv+), or both treatments (V+Mv+) in the epidermis and dermis layers of the skin.

A

Functional groups	N	Epidermis			Dermis		
		V+Mv-	V-Mv+	V+Mv+	V+Mv-	V-Mv+	V+Mv+
Cellular structures, processes and metabolism							
Chromosome	23	***1.17***	1.01	***1.65***	***1.94***	***1.41***	***1.65***
Cytoskeleton	29	1.10	0.94	***1.56***	***1.83***	***1.46***	***1.57***
Keratins	10	***1.23***	***1.16***	1.33	***1.78***	***2.51***	1.30
Microtubules	14	***1.26***	1.06	***2.05***	***2.38***	***1.70***	***1.99***
Motor proteins	8	***1.18***	1.01	***1.61***	***1.71***	1.48	***1.53***
Reticulum	13	***1.22***	1.01	***1.78***	***2.16***	***1.67***	***1.81***
Signaling	43	***1.26***	1.00	***1.88***	***1.98***	***1.49***	***1.87***
Transcription	22	***1.41***	***1.07***	***2.46***	***2.88***	***2.07***	***2.37***
Transcription factors	14	***1.30***	1.03	***2.10***	***2.53***	***1.73***	***1.98***
Protein folding	5	***1.49***	1.07	***2.52***	***3.22***	***2.01***	***3.10***
Amino acid metabolism	18	***1.23***	1.01	***1.90***	***2.08***	***1.59***	***1.97***
Calcium metabolism	17	1.17	-1.04	***1.80***	***2.43***	***1.87***	***1.88***
Eicosanoid metabolism	12	***1.26***	1.01	***1.86***	***2.02***	***1.56***	***1.83***
Ion metabolism	29	***1.27***	1.03	***2.01***	***2.16***	***1.61***	***1.84***
Lipid metabolism	54	***1.25***	1.01	***1.88***	***2.11***	***1.53***	***1.86***
Mitochondria	17	1.09	-1.12	***1.63***	***2.26***	***1.66***	***1.84***
Proteases	17	***1.29***	1.00	***1.62***	***1.46***	1.26	1.28
Steroid, bile metabolism	8	***1.20***	1.04	***1.73***	***1.80***	***1.47***	***1.61***
Sugar metabolism	25	0.77	***-1.49***	0.92	***1.92***	***1.31***	***1.28***
Transport	33	***1.23***	1.02	***1.97***	***2.34***	***1.69***	***1.97***
Ubiquitin	24	***1.28***	-1.01	***1.86***	***2.27***	***1.70***	***1.91***
Xenobiotic metabolism	12	***1.33***	1.10	***1.86***	***2.08***	***1.75***	***1.72***
Immune system and tissues							
Antivural response	50	***-1.64***	***-1.50***	***-1.47***	***-2.60***	***-2.05***	***-2.11***
Lymphocytes	12	-1.14	-1.12	-1.13	***-1.69***	***-1.50***	***-1.40***
Immune receptors	11	1.05	-1.01	-1.03	-1.44	***-1.48***	-1.28
Collagens	10	***1.22***	0.98	***1.58***	***2.00***	***1.47***	***1.62***
Differentiation	45	***1.17***	1.02	***1.63***	***1.67***	***1.31***	***1.47***
Differetiation-hox	12	***1.27***	1.01	***2.17***	***2.52***	***1.76***	***2.35***
Endocrine	20	***1.25***	1.04	***1.70***	***2.00***	***1.77***	***1.80***
Endothelium	6	***1.31***	1.02	***2.36***	***2.43***	***1.69***	***2.12***
Epithelium	11	***1.25***	0.98	***1.90***	1.67	1.39	***1.62***
Glycans	16	***1.23***	0.99	***1.58***	***1.74***	***1.41***	***1.60***
Growth factors	25	***1.21***	1.06	***1.81***	***1.82***	***1.46***	***1.58***
Mucus	25	***1.55***	***1.44***	***1.58***	***1.96***	***2.07***	***1.52***
Neural	69	***1.28***	***1.04***	***1.97***	***2.20***	***1.59***	***1.85***
Secretory	12	1.07	1.00	***1.73***	1.45	1.20	***1.72***

B

Genes	Epidermis			Dermis		
	V+Mv+	V-Mv+	V+Mv-	V+Mv-	V-Mv+	V+Mv+
Toll-like receptor 13	1.71	-1.03	1.20	***1.84***	1.44	1.57
C-X-C chemokine receptor type 5	1.56	1.04	1.23	***1.80***	1.51	1.72
LPS-induced TNFa-like (*D)	1.63	-1.03	-1.18	***2.58***	1.42	1.92
Interleukin-1 beta	***5.50***	1.13	1.93	***7.64***	3.35	***6.02***
IL-8 receptor (*E)	***2.84***	-1.05	***2.14***	1.38	-1.21	1.62
Interleukin-21	***2.71***	1.11	1.38	***3.33***	***2.35***	***2.73***
Granulins-like	***4.03***	1.15	1.80	1.33	***1.97***	1.53
Cytochrome P450 2K5	***2.51***	-1.05	1.45	***2.85***	***1.89***	***2.46***
Arachidonate 12-lipoxygenase	1.63	1.01	1.17	***1.78***	1.39	1.57
Leukotriene B4 receptor 1-like	***2.23***	1.02	1.24	***2.46***	1.68	***2.30***
Hydroperoxide isomerase ALOXE3	***1.98***	1.04	1.39	***2.62***	2.20	***2.00***
CD97 antigen-like (*D)	***1.77***	1.04	1.16	***2.65***	1.41	***2.78***
Complement C1q-like protein 2	1.38	1.02	1.19	***1.76***	1.54	1.63
Complement component c3a	***1.78***	1.04	1.29	***1.94***	1.44	***1.88***
Complement component 1q-like 3a	***1.92***	1.09	1.26	***1.97***	1.19	1.32
Cytochrome b-245 light chain	***6.41***	1.06	1.95	***9.41***	4.14	***7.48***
TNF alpha induced metalloreductase STEAP4	***2.88***	-1.01	1.41	***2.20***	1.51	***2.40***
Perforin-1-like (*D)	***1.86***	1.23	1.20	***2.71***	1.52	1.71
Perforin-1-like	1.17	1.35	1.33	1.22	***1.92***	1.83
MMP 13 or Collagenase 3 (*D)	***3.89***	-1.46	***3.22***	1.31	***-2.38***	***2.07***
Matrix metalloproteinase-9 (*D)	***2.28***	-1.18	***2.20***	1.20	***-1.86***	1.42
Collagenase 3-like (*D)	-1.66	2.22	1.10	***0.45***	1.14	***-1.99***
Barrier-to-autointegration factor (banf) (*D)	-1.19	-1.47	-2.30	***0.21***	-1.75	-2.83
Gig1-2	-2.12	-1.83	-2.05	***0.29***	-2.74	-2.65
Gig2-2	-1.90	-1.90	-2.14	***0.28***	-2.32	***-2.62***
Retinoic acid-inducible gene-I-1	-1.29	-1.28	-1.33	***0.46***	***-1.83***	***-2.07***
Very large inducible GTPase 1-2	-2.19	-2.09	***-2.52***	***0.23***	***-3.03***	-2.94
BCR-associated protein (CD79)	-1.47	-1.17	-1.21	***0.50***	-1.42	-1.69
B-cell linker protein-like	-1.20	-1.16	-1.04	***0.55***	-1.53	-1.50
B-cell receptor CD22-like-1	-1.18	1.07	-1.11	***0.50***	-1.50	***-1.77***
B-cell receptor CD22-like-2	-1.01	-1.15	-1.04	***0.54***	***-1.78***	-1.54
Tyrosine-protein kinase LCK	-1.34	-1.02	-1.06	***0.54***	-1.22	-1.65
CD3 epsilon	-1.51	-1.11	-1.21	***0.51***	-1.43	***-1.89***
CD4-like	-1.06	-1.05	1.25	0.56	***-2.23***	-1.64
CD8 alpha	-1.55	-1.18	-1.33	***0.54***	-1.18	-1.67
CD28 T-cell-specific surface glycoprotein	-1.49	-1.17	-1.31	***0.55***	-1.28	-1.59
Tyrosine-protein kinase ZAP-70	-1.40	-1.10	-1.15	***0.50***	-1.28	-1.68

Fig. 6. Microarray analyses of Atlantic salmon skin: differences to the unvaccinated and uninfected (V-Mv-) control group. (A) Functional groups (STARS annotation) with coordinated expression changes. The numbers of DEG are indicated. (B) Immune genes, each functional group is presented with no more than five DEG. Notations after gene names with (*E) and (*D) indicate significant difference between vaccinated and challenged fish (V+Mv- and V-Mv+) in epidermis and dermis. Data represent fold changes compared to V-Mv-. Differential expression is highlighted by underlined bold italics. Red and green colours denote up and down-regulation of expression. (For interpretation of the references to colour in this figure legend, the reader is referred to the web version of this article.)

scale pocket connective tissue, and curling of the scale tip. These findings correlated with weak staining using antibodies against *M. viscosa* and may be linked to early diagnostic markers of *M. viscosa* infection. Image analysis revealed that *M. viscosa* initiated infection by colonising the scale surface. The skin from fish with more developed pathogenesis showed prominent vacuolisation and infiltration of immune-related cells together with intense staining of *M. viscosa*. Tissue responses included the influx of blood and immune-related cells between the outer surface of the scale epidermis in addition to thickening of the epidermis and breakdown of the scales, and image analysis indicated disintegration of the epidermal layer from within.

It is believed that vaccination protects against pathogen mainly through mounting of specific antibodies. Ig-seq was included in this study due to recent discovery of the protective role of B cells recruitment to the infected sites as a marked increase in B cell trafficking followed by a subsequent reduction was observed in Atlantic salmon infected with salmonid alphavirus, an effect accelerated in vaccinated fish (Bakke et al., 2020). The present study did not find effect of vaccination nor *M. viscosa* that could be detected using Ig-seq. This was in line with minor overlap between IgM repertoire in skin and other tissues of Atlantic salmon. However, the transcriptomic analysis suggested egress of B and T cells from skin of vaccinated fish, which was reduced by infection with *M. viscosa*.

Difference of responses of the immune-related genes to inactivated (vaccine) and pathogenic *M. viscosa* was small, although a few genes showed stronger upregulation in vaccinated fish that was not challenged (V+Mv-). The lack of *M. viscosa* or pathogen-specific responses in the present trial could be related to an early infection stage at 4 dpi. This contrasts the strong transcriptional changes recently reported from RNAseq (Eslamloo et al., 2022) and microarray (Ramberg et al., 2022) data of the skin wound edge of *M. viscosa* ulcers. In the latter study, infection responsive miRNAs were also identified, but only associated with severe skin ulcers. Although the study designs were different, both used the edge of an ulcer that had penetrated the basement membrane up to 29- or 34-days post infection as the focused area of infection. Such infection sites would clearly be different from a stratified skin tissue layer. Indeed, Eslamloo et al., (2022) reported effects beyond the skin lesion site (~1 cm from the edge) to be subtle and more comparable to control samples. Initial skin ulcer areas with visible scales that still have epidermis and dermis layers intact, which has been the focus of this study, would likely resemble effects beyond the ulcer edge.

Skin layer-specific genes assist in the interpretation of gene profiles and elucidate the defensive roles of the epidermis and dermis, and have previously been reported from the outer skin (epidermis and scale) and inner skin (dermis) layers of Atlantic salmon (Sveen et al., 2021). In the present study, the transcriptional profiles suggested effects on calcium homeostasis that could indicate hypercalcemia. Pathogens may induce calcium release (Brunet et al., 2000; Asmat et al., 2014), leading to numerous effects, such as F-actin alteration (Brunet et al., 2000), which is also exerted by *M. viscosa* in cell models (Tunsjø et al., 2009). Image analysis revealed that this could be possible by *M. viscosa* colonising the scales and deteriorating the epidermis, creating a breach in the barrier between the epithelial layer and the seawater environment, which also applies for open wounds. Invading bacteria constantly battle with the host for transitional but essential metals that can be scavenged by bacterial siderophores, which *M. viscosa* also possess (Bjornsdottir et al., 2011; Hjerde et al., 2015). In response, an influx of blood or bleeding occurs and the host can respond using ferritins or heme-binding proteins (Hood and Skaar, 2012). The transcribed patterns of these genes were already at the level of infection in the immunised groups. Thus, the

A

Functional gene group	No. of genes	D/E fold
Erythrocyte, globins	25	6.7
Myofiber	142	6.3
Plasma proteins	38	4.7
Complement	20	4.3
Cytokines	6	3.6
Endothelium	29	3.2
Retinoid metabolism	25	3.1
Extracellular matrix	84	2.9
Mitochondria	66	2.7
Growth factors	75	2.6
Calcium metabolism	37	2.4
Differentiation	151	2.1
Sugar metabolism	65	2.0
Microtubules	17	1.9
Cytoskeleton	147	1.8
Collagens	83	1.6
Lectins	42	-0.5
Cell DNA replication	22	-1.6
Cell cycle	100	-1.7
Xenobiotic metabolism	39	-1.7
Chromosome maintenance	65	-1.8
Innate antiviral response	34	-1.9
T cells	35	-2.0
Cytochrome P450	13	-2.3
Mucus	52	-2.4
Keratin cytoskeleton	21	-2.4
Antigen presentation	19	-2.5

B

Gene	D/E fold
G0/G1 switch protein 2	457.2
Myosin, heavy chain b	200.5
Troponin T2d, cardiac	194.6
Antimicrobial peptide 2	166.7
Fibrinogen-like	129.0
Thrombospondin 4b	112.7
Thrombospondin-1	83.7
Retinol dehydrogenase 10	53.6
C type lectin receptor B	43.4
Creatine kinase, muscle a	43.3
Serotransferrin	37.5
Mannose-binding protein C	31.7
Thiamine triphosphatase	31.3
Retinoid-binding protein 7	30.8
Complement component C6	30.4
Complement component C4-B	22.3
C-C motif chemokine 17	21.7
Interleukin 17D	19.2
C1q TNF-related	17.8
Collagen type II, alpha-1a	14.8
Cytochrome P450 1A1	-10.9
Dnase gamma	-12.2
Keratin type I 17	-12.9
GMP Giant mucus protein	-13.6
Calpain 1	-17.3
Mucin 5B-2	-21.4
Mucin 5B-1	-24.5
C-type natriuretic peptide 1	-29.3
C-type natriuretic peptide 2	-34.8
WAP, Kazal, Ig, Kunitz, NTR-domain	-43.7

Fig. 7. Differences between transcriptomes in the epidermis and dermis. (A) Functional groups (STARS annotations), the number of differentially expressed genes are indicated. (B) Genes with the greatest expression differences. Data represent the dermis-to-epidermis fold (D/E fold). All results are significant ($P \leq 0.05$). Red and green colours denote up and down-regulation. (For interpretation of the references to colour in this figure legend, the reader is referred to the web version of this article.)

effect of immunisation could prime a protective response to infection beyond that of adaptive immunity. The transcriptional profiles of complement factors indicted that vaccination enhanced readiness to respond.

In fish, mediators of humoral immunity by vaccination could involve controlling metal homeostasis mechanisms, and regulation of inflammation and coagulation cascades (Braden et al., 2019). Several genes involved in the intrinsic coagulation pathway (phosphatidylinositol phospholipases, factor VIII and cofactor Ca^{2+}, von Willebrand factor, and thrombospondins and fibrinogens) were triggered in vaccinated and *M. viscosa*-challenged groups; therefore, all the necessary components are present in the blood. Acute mortality in Atlantic salmon in response to injected bacterial components was previously suggested to be associated with circulatory failure caused by bacterial-associated coagulation (Salte et al., 1992; Salte et al., 1993). *M. viscosa* infection can lead to external and internal haemorrhages with suspected final organ dysfunction. Clotting and thrombi throughout the vasculature consume large quantities of clotting factors, leading to increased risk of haemorrhaging (Davis et al., 2016). In mammals, development of severe infection could over-activate cascades into sepsis-associated disseminated intravascular coagulation and multiorgan failure (Patel et al., 2019); however, it is unclear whether this may also occur in fish during *M. viscosa* infection. If vaccination primes other features affecting immunity, such as a coagulation response, this could mediate more effective entrapment of the bacteria and prevent ulceration and later systemic dissemination.

Interestingly, microscopy combined with skin transcriptional profiling suggested that different skin layers were infected in the study groups, although both layers may be degraded by *M. viscosa*. In the dermis, the transcriptional profiles of vaccinated fish mimicked the action of the pathogen at a lower level. Vaccinated fish showed strong responses to the pathogen in the epidermis and minor responses in the dermis. The opposite was observed in unvaccinated fish, which showed minor responses in the epidermis but strong responses in the dermis. These findings were supported by the presence of *M. viscosa* in the different layers, as revealed by IHC. We propose that bacteria may have been trapped in the scale pocket layer of the skin of vaccinated salmon and induced similar transcriptional changes in the epidermis to those observed in the dermis (Fig. 8). In unvaccinated fish, bacteria populated the dermis layer, which may also explain why unvaccinated fish developed more ulcers during infection. Bacterial infection of the dermis layer of unvaccinated fish may also resolve the apparent paradox in the

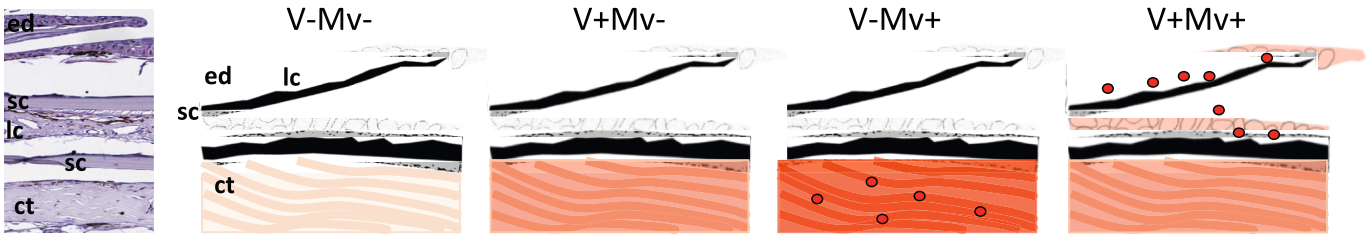

Fig. 8. Illustration of skin transcriptional profiles from vaccination and *M. viscosa* challenge. Expression changes are indicated by the intensity of the red colour. Vaccine and *M. viscosa* challenge (V+Mv+) induced similar changes in expression in the epidermis and the dermis, which were only seen in the dermis before *M. viscosa* challenge. After *M. viscosa* challenge, *M. viscosa* (red spots) resided in the dermis of unvaccinated salmon and in the scale pocket of vaccinated salmon, causing similar, although different by scale changes. Ed, epidermis; sc, scale; lc, loose connective tissue; ct, connective tissue. (For interpretation of the references to colour in this figure legend, the reader is referred to the web version of this article.)

microarray data that indicated that the epidermis responded to combined (V+Mv+) but not individual treatment (V+Mv- or V-Mv+). Interestingly, the same functional groups and genes responded to the pathogen in the epidermis and dermis of vaccinated salmon, despite profound differences between the transcriptomes of the skin layers.

5. Conclusions

The present study revealed that the use of variant *M. viscosa* in the vaccination formula may improve vaccination against winter ulcers. Specific antibody levels are unknown and our performed Ig-seq was not able to show effect of vaccination or *M. viscosa* challenge on antibody repertoire and B cell trafficking from the lymphatic organs to skin. Skin transcriptional analysis suggested instead egress of B and T cells from the skin of vaccinated fish, which was reduced by infection with *M. viscosa*. Detected skin transcriptional immune responses to vaccine and live *M. viscosa* were limited but similar and included up-regulation of proinflammatory genes. It is suggested that *M. viscosa* initiates infection by scale surface colonisation, which evolved differently between the study groups. *M. viscosa* was most likely harboured in the epidermis layer of vaccinated salmon and colonised the dermis of unvaccinated fish, which could suggest why unvaccinated fish develop greater ulceration. We propose that i.p. vaccination may prime the humoral innate response and pre-activation of this response facilitates a rapid response in the dermis of skin during bacterial invasion.

Author contributions

CK planned and executed the study design, sampling and drafting the paper. EY and LS performed immunohistological, histological and scanning electron microscopy analysis. AF, ST, MGT planned and executed the study design, prepared bacterial cultures and vaccinations. SA and AK performed transcriptomic data and statistical analysis. All co-authors reviewed, edited, and approved the final manuscript.

Funding

This study was supported by the Research Council of Norway through CtrlAQUA SFI (project 237856/O30). SA was supported by the Sechenov Institute of Evolutionary Physiology and Biochemistry of RAS, the State assignment No. 075-00967-23-00.

Ethics statement

The study was approved by the Norwegian Food Safety Authority and conducted in accordance with the regulations controlling experiments and procedures for live animals in Norway.

Declaration of Competing Interest

AF, ST, MGT are employed by the Pharmaq part of Zoetis. The remaining authors declare that the research was conducted in the absence of any commercial or financial relationships that could be construed as a potential conflict of interest.

Data availability

Data will be made available on request.

References

Asmat, T.M., Tenenbaum, T., Jonsson, A.-B., Schwerk, C., Schroten, H., 2014. Impact of calcium signaling during infection of *Neisseria meningitidis* to human brain microvascular endothelial cells. PLoS One 9 (12), e114474. https://doi.org/10.1371/journal.pone.0114474.

Bakke, A.F., Bjørgen, H., Koppang, E.O., Frost, P., Afanasyev, S., Boysen, P., et al., 2020. IgM+ and IgT+ B cell traffic to the heart during SAV infection in Atlantic salmon. Vaccines (Basel) 8 (3). https://doi.org/10.3390/vaccines8030493.

Benediktsdottir, E., Helgason, S., Sigurjonsdottir, H., 1998. *Vibrio* spp. isolated from salmonids with shallow skin lesions and reared at low temperature. J. Fish Dis. 21 (1), 19–28.

Benediktsdottir, E., Verdonck, L., Sproer, C., Helgason, S., Swings, J., 2000. Characterization of *Vibrio viscosus* and *Vibrio wodanis* isolated at different geographical locations: a proposal for reclassification of *Vibrio viscosus* as *Moritella viscosa* comb. nov. Int. J. Syst. Evol. Microbiol. 50, 479–488.

Bjornsdottir, B., Fridjonsson, O.H., Magnusdottir, S., Andresdottir, V., Hreggvidsson, G. O., Gudmundsdottir, B.K., 2009. Characterisation of an extracellular vibriolysin of the fish pathogen *Moritella viscosa*. Vet. Microbiol. 136 (3–4), 326–334.

Bjornsdottir, B., Gudmundsdottir, T., Gudmundsdottir, B.K., 2011. Virulence properties of *Moritella viscosa* extracellular products. J. Fish Dis. 34 (5), 333–343.

Braden, L.M., Whyte, S.K., Brown, A.B.J., Iderstine, C.V., Letendre, C., Groman, D., et al., 2019. Vaccine-induced protection against furunculosis involves pre-emptive priming of humoral immunity in Arctic charr. Front. Immunol. 10 https://doi.org/10.3389/fimmu.2019.00120.

Brunet, J.P., Cotte-Laffitte, J., Linxe, C., Quero, A.M., Géniteau-Legendre, M., Servin, A., 2000. Rotavirus infection induces an increase in intracellular calcium concentration in human intestinal epithelial cells: role in microvillar actin alteration. J. Virol. 74 (5), 2323–2332. https://doi.org/10.1128/jvi.74.5.2323-2332.2000.

Bruno, D.W., Griffiths, J., Petrie, J., Hastings, T.S., 1998. *Vibrio viscosus* in farmed Atlantic salmon *Salmo salar* in Scotland: field and experimental observations. Dis. Aquat. Org. 34 (3), 161–166.

Castro, R., Navelsaker, S., Krasnov, A., Du Pasquier, L., Boudinot, P., 2017. Describing the diversity of ag specific receptors in vertebrates: contribution of repertoire deep sequencing. Dev. Comp. Immunol. https://doi.org/10.1016/j.dci.2017.02.018.

Davis, R.P., Miller-Dorey, S., Jenne, C.N., 2016. Platelets and coagulation in infection. Clin. Transl. Immunol. 5 (7), e89. https://doi.org/10.1038/cti.2016.39.

Eslamloo, K., Kumar, S., Xue, X., Parrish, K.S., Purcell, S.L., Fast, M.D., et al., 2022. Global gene expression responses of Atlantic salmon skin to *Moritella viscosa*. Sci. Rep. 12 (1), 4622. https://doi.org/10.1038/s41598-022-08341-7.

Greger, E., Goodrich, T., 1999. Vaccine development for winter ulcer disease, *Vibrio viscosus*, in Atlantic salmon, *Salmo salar* L. J. Fish Dis. 22 (3), 193–199. https://doi.org/10.1046/j.1365-2761.1999.00163.x.

Grove, S., Wiik-Nielsen, C.R., Lunder, T., Tunsjø, H.S., Tandstad, N.M., Reitan, L.J., et al., 2010. Previously unrecognised division within *Moritella viscosa* isolated from fish farmed in the North Atlantic. Dis. Aquat. Org. 93 (1), 51–61.

Heidarsdóttir, K.J., Gravningen, K., Benediktsdóttir, E., 2008. Antigen profiles of the fish pathogen *Moritella viscosa* and protection in fish. J. Appl. Microbiol. 104 (4), 944–951. https://doi.org/10.1111/j.1365-2672.2007.03639.x.

Hjerde, E., Karlsen, C., Sørum, H., Parkhill, J., Willassen, N.P., Thomson, N.R., 2015. Co-cultivation and transcriptome sequencing of two co-existing fish pathogens *Moritella viscosa* and *Aliivibrio wodanis*. BMC Genomics 16 (1), 447–459.

Hood, M.I., Skaar, E.P., 2012. Nutritional immunity: transition metals at the pathogen-host interface. Nat. Rev. Microbiol. 10 (8), 525–537. https://doi.org/10.1038/nrmicro2836.

Jenberie, S., Thim, H.L., Sunyer, J.O., Skjødt, K., Jensen, I., Jørgensen, J.B., 2018. Profiling Atlantic salmon B cell populations: CpG-mediated TLR-ligation enhances IgM secretion and modulates immune gene expression. Sci. Rep. 8 (1), 3565. https://doi.org/10.1038/s41598-018-21895-9.

Karlsen, C., Ellingsen, A.B., Wiik-Nielsen, C., Winther-Larsen, H.C., Colquhoun, D., Sørum, H., 2014a. Host specificity and clade dependent distribution of putative virulence genes in *Moritella viscosa*. Microb. Pathog. 77 (0), 53–65.

Karlsen, C., Vanberg, C., Mikkelsen, H., Sorum, H., 2014b. Co-infection of Atlantic salmon (*Salmo salar*), by *Moritella viscosa* and *Aliivibrio wodanis*, development of disease and host colonization. Vet. Microbiol. 171, 112–121.

Karlsen, C., Hjerde, E., Klemetsen, T., Willassen, N.P., 2017a. Pan genome and CRISPR analyses of the bacterial fish pathogen *Moritella viscosa*. BMC Genomics 18 (1), 313. https://doi.org/10.1186/s12864-017-3693-7.

Karlsen, C., Thorarinsson, R., Wallace, C., Salonius, K., Midtlyng, P.J., 2017b. Atlantic salmon winter-ulcer disease: combining mortality and skin ulcer development as clinical efficacy criteria against *Moritella viscosa* infection. Aquaculture 473, 538–544. https://doi.org/10.1016/j.aquaculture.2017.01.035.

Krasnov, A., Timmerhaus, G., Afanasyev, S., Jørgensen, S.M., 2011. Development and assessment of oligonucleotide microarrays for Atlantic salmon (*Salmo salar* L.). Comp. Biochem. Physiol. Part D Genomics Proteomics 6 (1), 31–38. https://doi.org/10.1016/j.cbd.2010.04.006.

Krasnov, A., Jorgensen, S.M., Afanasyev, S., 2017. Ig-seq: deep sequencing of the variable region of Atlantic salmon IgM heavy chain transcripts. Mol. Immunol. 88, 99–105. https://doi.org/10.1016/j.molimm.2017.06.022.

Lunder, T., Evensen, O., Holstad, G., Hastein, T., 1995. Winter ulcer in the Atlantic salmon *Salmo salar* - pathological and bacteriological investigations and transmission experiments. Dis. Aquat. Org. 23 (1), 39–49.

Lunder, T., Sørum, H., Holstad, G., Steigerwalt, A.G., Mowinckel, P., Brenner, D.J., 2000. Phenotypic and genotypic characterization of *Vibrio viscosus* sp. nov. and *Vibrio wodanis* sp. nov. isolated from Atlantic salmon (*Salmo salar*) with 'winter ulcer'. Int. J. Syst. Evol. Microbiol. 50 (2), 427–450.

Makesh, M., Sudheesh, P.S., Cain, K.D., 2015. Systemic and mucosal immune response of rainbow trout to immunization with an attenuated *Flavobacterium psychrophilum* vaccine strain by different routes. Fish Shellfish Immunol. 44 (1), 156–163. https://doi.org/10.1016/j.fsi.2015.02.003.

Olsen, A.B., Nilsen, H., Sandlund, N., Mikkelsen, H., Sørum, H., Colquhoun, D.J., 2011. *Tenacibaculum* sp. associated with winter ulcers in sea-reared Atlantic salmon *Salmo salar*. Dis. Aquat. Org. 94 (3), 189–199.

Patel, P., Walborn, A., Rondina, M., Fareed, J., Hoppensteadt, D., 2019. Markers of inflammation and infection in sepsis and disseminated intravascular coagulation. Clin. Appl. Thromb. Hemost. 25 https://doi.org/10.1177/1076029619843338, 1076029619843338-1076029619843338.

Piazzon, M.C., Galindo-Villegas, J., Pereiro, P., Estensoro, I., Calduch-Giner, J.A., Gómez-Casado, E., et al., 2016. Differential modulation of IgT and IgM upon parasitic, bacterial, viral, and dietary challenges in a perciform fish. Front. Immunol. 7, 637. https://doi.org/10.3389/fimmu.2016.00637.

Ramberg, S., Krasnov, A., Colquhoun, D., Wallace, C., Andreassen, R., 2022. Expression analysis of *Moritella viscosa*-challenged Atlantic salmon identifies disease-responding genes, microRNAs and their predicted target genes and pathways. Int. J. Mol. Sci. 23 (19), 11200.

Salte, R., Norberg, K., Arnesen, J.A., Ødegaard, O.R., Eggset, G., 1992. Serine protease and glycerophospholipid:cholesterol acyltransferase of *Aeromonas salmonicida* work in concert in thrombus formation; in vitro the process is counteracted by plasma antithrombin and α2-macroglobulin, 15 (3), 215–227. https://doi.org/10.1111/j.1365-2761.1992.tb00658.x.

Salte, R., Norberg, K., Ødegaard, O.R., Arnesen, J.A., Olli, J.J., 1993. Exotoxin-induced consumptive coagulopathy in Atlantic salmon, *Salmo salar* L.: inhibitory effects of exogenous antithrombin and α2-macroglobulin on *Aeromonas salmonicida* serine protease, 16 (5), 425–435. https://doi.org/10.1111/j.1365-2761.1993.tb00876.x.

Småge, S.B., Frisch, K., Vold, V., Duesund, H., Brevik, Ø.J., Olsen, R.H., et al., 2018. Induction of tenacibaculosis in Atlantic salmon smolts using *Tenacibaculum finnmarkense* and the evaluation of a whole cell inactivated vaccine. Aquaculture 495, 858–864. https://doi.org/10.1016/j.aquaculture.2018.06.063.

Sommerset, I., Jensen, B.B., Bornø, G., Haukaas, A., Brun, E., 2021. The health situation in Norwegian aquaculture 2020. Norwegian Vet. Inst. (ISSN 1890-3290).

Sveen, L., Karlsen, C., Ytteborg, E., 2020. Mechanical induced wounds in fish – a review on models and healing mechanisms. Rev. Aquac. https://doi.org/10.1111/raq.12443.

Sveen, L., Krasnov, A., Timmerhaus, G., Bogevik, A.S., 2021. Responses to mineral supplementation and salmon lice (*Lepeophtheirus salmonis*) infestation in skin layers of Atlantic salmon (*Salmo salar* L.). Genes 12 (4), 602.

Tunsjø, H.S., Paulsen, S.M., Berg, K., Sørum, H., L'Abee-Lund, T.M., 2009. The winter ulcer bacterium *Moritella viscosa* demonstrates adhesion and cytotoxicity in a fish cell model. Microb. Pathog. 47 (3), 134–142.

Tunsjø, H.S., Wiik-Nielsen, C.R., Grove, S., Skjerve, E., Sørum, H., L'Abee-Lund, T.M., 2011. Putative virulence genes in *Moritella viscosa*: activity during *in vitro* inoculation and *in vivo* infection. Microb. Pathog. 50 (6), 286–292.

Whitman, K.A., Backman, S., Benediktsdottir, E., Coles, M., Johnson, G., 2000. Isolation and characterization of a new *Vibrio* spp. (*Vibrio wodanis*) associated with winter ulcer disease in sea water raised Atlantic salmon (*Salmo salar* L.) in New Brunswick. Aquacult. Assoc. Canada 4, 115–117. SpecialPublication.

Ye, J., Coulouris, G., Zaretskaya, I., Cutcutache, I., Rozen, S., Madden, T.L., 2012. Primer-BLAST: a tool to design target-specific primers for polymerase chain reaction. BMC Bioinformatics 13 (1), 134. https://doi.org/10.1186/1471-2105-13-134.